Journal of Chromatography A, 1217 (2010) 7891–7897

Contents lists available at ScienceDirect

Journal of Chromatography A

journal homepage: www.elsevier.com/locate/chroma

Single walled carbon nanotube length determination by asymmetrical-flow field-flow fractionation hyphenated to multi-angle laser-light scattering

Julien Gigault, Isabelle Le Hécho, Stéphane Dubascoux, Martine Potin-Gautier, Gaëtane Lespes*

Université de Pau et des Pays de l'Adour (UPPA)/CNRS, Laboratoire de Chimie Analytique Bio-Inorganique et Environnement, UMR IPREM 5254, Technopôle Hélioparc, Av. du Président Angot, 64000 PAU, France

ARTICLE INFO

Article history:
Received 13 January 2010
Received in revised form 9 September 2010
Accepted 11 October 2010
Available online 15 October 2010

Keywords:
SWCNT
Size fractionation
Length measurement
Hyphenated technique

ABSTRACT

Asymmetrical flow field-flow fractionation (AFlFFF) hyphenated to multi-angle laser-light scattering (MALS) was evaluated in order to determine single walled carbon nanotube (SWCNT) length distribution. Fractionation conditions were investigated by examining mobile phase ionic strength and pH, channel components and cross-flow rate. Ammonium nitrate-based mobile phase with 10^{-5} mol L^{-1} ionic strength and pH 6 allows the highest sample recovery ($89 \pm 3\%$) to be obtained and the lowest loss of the longest SWCNT. A cross-flow rate of 0.9 mL min^{-1} leads to avoid any significant membrane–sample interaction. Length was evaluated from gyration radius measured by MALS by comparing SWCNT to prolate ellipsoid. In order to validate the fractionation and the length determination obtained by AFlFFF-MALS, different SWCNT aliquots were collected after fractionation and measured by dynamic light scattering (DLS). AFlFFF is confirmed to operate in normal mode over 100–2000 nm length. MALS length determination after fractionation is found to be accurate with 5% RSD. Additionally, a shape analysis was performed by combining gyration and hydrodynamic radii.

1. Introduction

For more than 10 years, manufactured nanoparticles have driven the attention of a large part of the scientific community. The most known of them are carbon nanotubes (CNT), which represent a new industrial revolution. Carbon nanotubes show great potential for material applications including electronics, sensors, field emission devices, batteries/fuel cells, fibers/reinforced composites, medicine/biology, catalysis and gas storage [1]. They combine particular electronic structures, high surface area, electrical conductivity and excellent strength. Single walled carbon nanotubes (SWCNT) are rodlike molecular objects with diameter and length of about 0.5–5 nm and 100 nm to 200 μm, respectively. They have a structure of a rolled graphene sheet and roll-up vector direction determines their chirality and diameter.

Due to SWCNT complexity and heterogeneity, one of the major challenges in analytical chemistry is their size characterisation (i.e. diameter and length) and the determination of their electronic properties. The capability to obtain CNT size distribution is becoming essential in order to improve and control their manufacturing processes and better understand their environmental impacts. SWCNT characterisation can be carried out by two types of analytical techniques. The first one based on physical fractionation is able to produce size distribution of CNT sample. The second one spectroscopic or microscopic-based gives average size data.

Fractionation of SWCNT according to their size can be achieved through several techniques such as size exclusion chromatography (SEC), gel electrophoresis (GE), capillary electrophoresis (CE) or field-flow-fractionation (FFF). Recent studies have shown that SEC can lead to a reasonable size-resolution of SWCNT [2–6]. However, the exclusion limit of the SEC column, controlled by the pore size, restricts the SWCNT that can be separated to those shorter than 1 μm. Doorn et al. [7] showed that CE can be used to separate SWCNT according to their length but the size resolution remains low and the quantity separated small by comparison with SEC. CNT FFF-based fractionation is reported in aqueous dispersions [8–12]. Some of these studies refer to SWCNT separation by flow field-flow fractionation (FlFFF) [8,9]. The results show that FlFFF is a promising technique due to its versatility and its size-resolution potential. It can be used as separation and purification process as well as length characterisation technique when hyphenated to appropriate detector (see later on). Nevertheless no optimisation of FlFFF SWCNT fractionation investigating some crucial operating factors such as mobile phase, channel components and cross-flow has been still performed up to now. Currently, no information about sample recovery after fractionation or even fractionation

* Corresponding author. Tel.: +33 559407671.
E-mail address: gaetane.lespes@univ-pau.fr (G. Lespes).

0021-9673/$ – see front matter © 2010 Elsevier B.V. All rights reserved.
doi:10.1016/j.chroma.2010.10.042

repeatability is available, making FlFFF-based procedure difficult to validate.

Other analytical techniques allow SWCNT to be physico-chemically characterized. Spectroscopic techniques such as absorption (UV–vis and near-infrared) and Raman are weakly affected by aggregation but do not provide any quantitative length-measurement [13–15]. Fluorescence spectroscopy detects semiconducting SWCNT that are not in ropes or tight bundles, but it is not sensitive enough to detect the presence of conducting nanotubes [14]. Atomic force, scanning, and transmission microscopies (AFM, SEM and TEM) only focus on a small part of nanotube sample. Bias measurement can occur during sample preparation if all tube types are not equally deposited on the visible field especially in case of diluted samples [13]. Static and dynamic light scattering detection can intrinsically provide information on the size of nanoparticles (i.e. gyration and hydrodynamic radii, R_g and R_h, respectively). Studies based on static light scattering such as multi-angle laser light scattering (MALS) were reported on SWCNT/deoxyribonucleic acid (DNA) dispersions and showed that SWCNT bundles from individually dispersed ones can be differentiated by this technique [16,17]. Another work reported SWCNT length characterisation after fractionation by using FlFFF [9]. In this paper, in order to prevent the important dilution induced during the fractionation and so to be over MALS limits of detection, the authors prepared SWCNT dispersion with concentrations in the range of some hundred mg L^{-1}. In these conditions, some anomalous concentration-dependent signals were observed suggesting the presence of possible bundles or aggregates.

Despite the great deal of interest for nanoparticle characterisation, there is yet a need for a qualitative and quantitative method able to provide a relevant size-characterisation from nanotube dispersions. For example, individual length evaluation is crucial information for nanotechnology. One interesting analytical strategy consists of the hyphenation of an on-line fractionation to one or several complementary detectors in order to obtain size distribution associated to size measurement. Unfortunately up to now, there is no paper investigating the potentiality of FlFFF-MALS coupling to the accurate length determination associated with a validation analytical approach.

Considering this lack of characterisation tool, the objective of this work was to evaluate the capabilities of asymmetrical flow field-flow fractionation (AFlFFF) hyphenated to MALS for accurately measuring SWCNT length from aqueous dispersions. Diluted samples were considered in order to obtain the size-resolution as high as possible and try to achieve individual nanotube elution. Fractionation was performed by AFlFFF, which offers less dilution, shorter analysis duration and easier instrument maintenance and control compared to symmetrical system previously used [8,9,18]. Despite such approach is very attractive, it was never investigated before. Fractionation key parameters were investigated to have a method robust enough for heterogeneous sample. On-line MALS analysis of the eluted SWCNT was used to check the recovery and determine length distribution. In order to evaluate the separation effectiveness and the accuracy of the associated size information of AFlFFF-MALS coupling, different SWCNT aliquots were collected after AFlFFF fractionation. Their hydrodynamic radii (R_h) were measured by dynamic light scattering (DLS) as R_h value directly depends on size-fractionation. Thus DLS measurements allowed the fractionation as well as size determination to be controlled. Complementary, MALS analysis in the bulk dispersion was achieved in order to check AFlFFF fractionation reliability. This validation approach based on light scattering detectors was preferred to the use of microscopy because the sample dilution leads to have concentration lower than limits of detection of microscopic techniques [12].

2. Experimental

2.1. Chemical

Ammonium nitrate (NH_4NO_3, 99.5%) and sodium dodecyl sulfate (SDS, 98.5%) were purchased from Sigma–Aldrich. Sodium hydroxide (NaOH, 99%) used to adjust mobile phase pH was purchased from Merck (Merck, Darmstadt, Germany).

Latex nanospheres came from Duke Scientific Corp (Microgenics Corporation, Fremont, CA, USA). The water used was Milli-Q 18 MΩ (Millipore System, Bedford, MA, USA). Filters used for carrier were Durapore 0.1 μm from Millipore.

For sample filtration, syringe filters (Minisart) with 5.0 μm pore size were purchased from VWR (Whatman, Dassel, Germany).

SWCNT were purchased from Sigma–Aldrich (numbered lot from Sigma–Aldrich, St Quentin Fallaire, France). According to the manufacturer, the SWCNT size characteristics are: diameter of 1.3 ± 0.3 nm; lengths from <500 up to 2000 nm (obtained from independent measurements by Raman and SEM techniques). These lengths were considered as indicative values later on.

2.2. Sample

Aqueous dispersion of SWCNT in the presence of SDS was considered as a test sample. It was prepared by adding SWCNT powder in SDS aqueous solution, the suspension obtained being then sonicated. In order to optimize the AFlFFF SWCNT fractionation, all experiments were made on the test sample filtered at 5.0 μm. This filtration cut-off allows the whole SWCNT length range given by the manufacturer to be covered and the possible bulk impurities to be removed. The final SWCNT concentration was 0.01 g L^{-1}. The whole procedure of preparation was previously validated. Thus, length values given by the manufacturer were considered as reference values since preparation step does not induce any significant change in length range [19].

Duke nanospheres (40, 80, 200 and 300 nm in hydrodynamic radii) were diluted in Milli-Q water in order to obtain size-standard solutions with a detectable MALS signal.

2.3. Instruments

The asymmetrical flow field-flow fractionation system was an Eclipse 3 (Wyatt Technology, Dernbach, Germany). The trapezoidal-shape channel dimensions were 26.5 cm in length, and, respectively, 0.6 and 2.1 cm in width. For the experiments, different spacers (from 190 to 350 μm thickness) and different membranes (cellulose triacetate, polyethersulfone and regenerated cellulose) were tested. Flows rates were controlled with an Agilent Technologies 1100 series isocratic pump equipped with a micro-vacuum degasser. MALS detector was a multi-angle laser-light scattering DAWN HELEOS (Wyatt Technology, Santa Barbara, USA). All injections were performed with an autosampler (Agilent Technologies 1100 series). Data from MALS detector were collected and treated with Astra 5.3.1.5 software (Wyatt Technology). The gyration (R_g) and hydrodynamic (R_h) radii were measured for carbon nanotubes and Duke Nanospheres. The gyration radius was obtained using Zimm first-order fit formalism for SWCNT as it is the best way of calculation for non-spherical particles whereas sphere fit method was used for Duke nanosphere radius calculation [20,21]. Rodlike formalism that allows the direct evaluation of particle length was also preliminary considered for nanotubes. For SWCNT Zimm fit method was used at sufficient small angles (found to be $\leq 90°$) in order to be in conditions of no analyte-shape dependence as previously demonstrated elsewhere [22]. Additionally, the fitting accuracy was controlled by plotting the SWCNT scattering function from various selections of small angles up to all the MALS angles. Typical

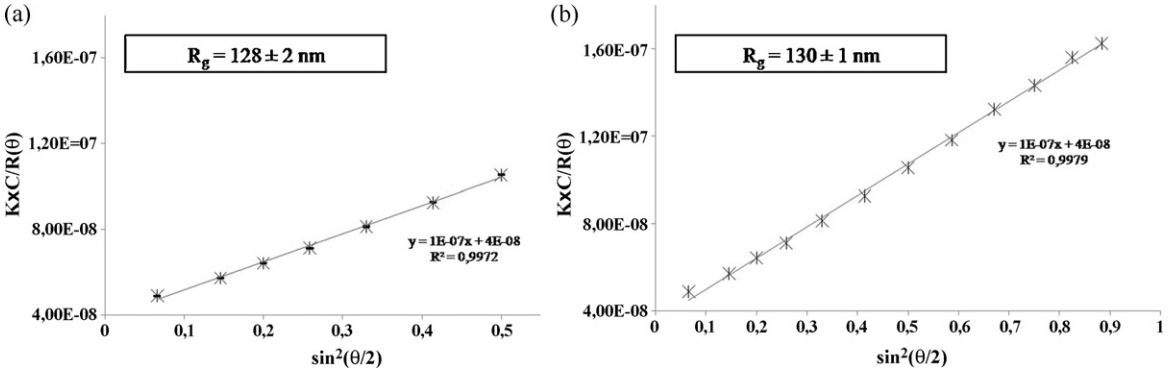

Fig. 1. Zimm fit method with: (a) angles ≤90° and (b) all angles of SWCNT MALS signal for peak region corresponding to $R_g \approx 130$ nm.

results obtained are presented in Fig. 1. This approach allows the relevance for using the selected angles used in this paper to be verified. The hydrodynamic radius of the SWCNT was obtained from dynamic light scattering (DLS) (Zetasizer, Malvern instrument, London, UK) by using CONTIN-based algorithm as it was previously described as relevant for non-spherical particles [23].

2.4. Fractionation conditions

The mobile phase was an aqueous solution containing NH_4NO_3. For the optimisation, various ionic strengths were tested from 0 to 10^{-3} mol L^{-1}, with various pH ranging from 6 to 8. The injection flow rate during the focus step was adjusted at 0.2 mL min^{-1}. The run sequences first contained two short and consecutive steps of elution and focussing without injection to equilibrate the system and follow the signal baseline. Different cross-flow rates were tested, from 0.3 to 1.2 mL min^{-1}, in order to obtain convenient SWCNT fractionation. At the end of the fractionation process, a rinse step without cross-flow was applied. Each run was replicated 6 times in order to calculate experimental uncertainties.

2.5. Analytical setup

Different equations were used to evaluate the effectiveness and quality of analyte fractionation [18,24]. First the recovery from an AFlFFF run, i.e. the ratio between recovered mass after analysis and injected mass, was expressed as:

$$R(\%) = \frac{S}{S_0} \times 100 \quad (1)$$

with S and S_0: the peak areas obtained with and without cross-flow, respectively.

Fractionation in FlFFF normal mode was determined by the diffusion coefficient of the analytes and thereby by their hydrodynamic radius R_h. The formula (2) links R_h to the retention parameter R according to [18]:

$$R_h = \frac{kTV_0(1-R)^{1/3}}{\pi\eta V_c w^2 R} \quad (2)$$

with V_0 the void volume, V_c the cross-flow, η the viscosity of the mobile phase, R the retention parameter defined as t_0/t_R (ratio between void and retention times), w the channel thickness (m) and k the Boltzmann constant. When V_c is kept constant and t_R sufficiently long (meaning $t_0/t_R \ll 1$) the formula (2) could be simplified in a linear relationship between R_h and t_R:

$$R_h = A \times t_R \quad (3)$$

with A being assumed to be constant under constant operating conditions.

Selectivity, defined as the intrinsic fractionation capability of the FFF method, was size-based evaluated and calculated according to:

$$S_d = \left| \frac{d(\log t_R)}{d(\log d_h)} \right| \quad (4)$$

with d_h the hydrodynamic diameter (=$2 \times R_h$).

In order to evaluate SWCNT size and shape from MALS data (i.e. R_g) the following calculation approach was considered. Carbon nanotubes were assumed to be prolate ellipsoids as this modelling was previously validated by Phelan and Bauer [25]. Especially these authors have demonstrated the relevance of such modeling with regard to SWCNT Brownian dynamics in cross-flow driven FlFFF channel, in a range of aspect ratio over 10–1000. Prolate ellipsoid was also preferred to rodlike since (1) Green et al. have showed that significant differences exist between SWCNT and rigid rod objects, (2) Monsfield and Douglas have highlighted that rodlike formalism is not the most appropriate for modeling carbon nanotube transport [26,27]. Additionally, preliminary comparative length calculations were performed by using on one hand Zimm formalism associated to prolate ellipsoid modeling (calculation details are presented later on) and on the other hand rodlike formalism. Rodlike-based length values were found to be twice as small as lengths obtained from Zimm/prolate for the longest SWCNT. Length underestimate can be attributed to the facts that (1) rodlike formalism does not consider mass distribution inside particle (i.e. nanotube) and (2) high aspect ratio as well as flexibility are better taken into account by prolate ellipsoid modeling [27]. This observation confirms that the joint use of Zimm formalism and prolate ellipsoid appears as the most convenient. Thus this approach was used later on.

On the basis on a sphere defined as an ellipsoid with its half axes $a = b = c$, a prolate ellipsoid is such as $a > b = c$, $2a$ corresponding to the SWCNT length (L) and $2b$ to the SWCNT diameter (d). On the one hand, the general relationship between the gyration radius and the half axes of an ellipsoid is [28,29]:

$$R_g = \sqrt{\frac{a^2 + b^2 + c^2}{5}} \quad (5)$$

This equation can be also expressed according to the SWCNT length and diameter:

$$R_g = \sqrt{\frac{L^2 + 2d^2}{20}} \quad (6)$$

For the SWCNT test sample and according to the manufacturer data, $d \ll L$. So, d can be neglected compared to L and Eq. (6) rewritten as:

$$L = R_g \times \sqrt{20} \quad (7)$$

On the other hand, diffusion coefficient (D_{diff}) of a prolate ellipsoid can also be expressed as a function of length and diameter of

Table 1
SWCNT recoveries $R(\%)$ calculated from Eq. (1) for different salt concentrations and pH of the mobile phase.

pH	NH_4NO_3 concentrations			
	0 mol L^{-1}	1×10^{-5} mol L^{-1}	5×10^{-4} mol L^{-1}	1×10^{-3} mol L^{-1}
6.1 ± 0.2	83 ± 1	93 ± 1	16.0 ± 0.3	2.2 ± 0.5
7.2 ± 0.2	72.0 ± 0.5	70 ± 2	45.1 ± 0.2	16.8 ± 0.4
8.0 ± 0.1	81.2 ± 0.2	81.1 ± 0.6	50 ± 2	36 ± 1

the ellipsoid according to Perrin [30]:

$$D_{\text{diff}} = \frac{kT}{3\pi\eta L\sqrt{1-(d/L)^2}} \ln\left[\frac{1+\sqrt{1-(d/L)^2}}{(d/L)}\right] \quad (8)$$

According to Stokes–Einstein equation, diffusion coefficient and hydrodynamic radius are linked by [18]:

$$R_h = \frac{kT}{6\pi\eta D_{\text{diff}}} \quad (9)$$

Combining (8) and (9), it can be obtained:

$$R_h = \frac{(L/2)\sqrt{1-(d/L)^2}}{\ln[(1+\sqrt{1-(d/L)^2})/(d/L)]} \quad (10)$$

This expression is in agreement with this one given by Schurtenberg and Newman in the hypothesis of prolate ellipsoid [31]. This equation can be also simplified by considering that $d = 1.3 \pm 0.3$ nm and $d \ll L$. Thus it can be rewritten as:

$$R_h = \frac{L/2}{\ln(2L/d)} \quad (11)$$

Finally, from Eqs. (6) and (10), and when d has a known value sufficiently inferior to L (typically $d/L \leq 1$–2%), R_h can be expressed as a function of R_g and d only, as it can be deduced from Eqs. (7) and (11):

$$R_h = \frac{\sqrt{5}R_g}{\ln[2\sqrt{20}R_g/d]} \quad (12)$$

Statistical tests were performed in a 95% confidence interval (i.e. $\alpha = 0.05$). Linear curves, plotted from n experimental data (x_i, y_i) ($i = 1$ to n, $n = 4$ in the present study), were validated by considering three criteria: precision, signification and lack of bias. Precision was evaluated by the determination coefficient, R^2. Signification was checked by a Fisher–Snedecor test ($F_{\text{obs}} = ((n-2)R^2)/(1-R^2)$, which has to be higher than the reference value $F_{\alpha,1,n-1}$ in order to have a significant fitting). Lack of bias was controlled by plotting the n residues $e_i = y_i - f(x_i)$, which are to be no auto-correlated (i.e. no fitting possible between them).

Homogeneity of the mean values of two sets of data was evaluated in order to check if these mean values are statistically equal or not. It was checked by a Student test involving the mean values of these sets of data number and their corresponding variances.

3. Results and discussion

3.1. Determination of fractionation conditions

The aim of this part is to find the operating conditions giving an efficient separation without any loss due to size-discrimination. For that, three criteria have to be considered: the recovery ($R\%$), the SWCNT size range and the retention times. SWCNT length has to be distributed over the maximum range and correspond to the manufacturer length data. Fractionation is effective when sufficient retention time is achieved, i.e. retention time such that elution over the void volume and retention ratio $R \ll 1$.

3.1.1. Mobile phase

Mobile phase is crucial in flow field-flow fractionation because its salt nature, ionic strength and pH could directly influence particle stability and increase or decrease interactions with the membrane [24].

Concerning salt nature, it has been shown that monovalent salt has no influence on the recovery of various colloidal samples fractionated [24]. So, NH_4NO_3 was chosen for the present investigation because it allows the mobile phase to be compatible with various detectors in the perspective of a multi-detection approach (e.g. involving atomic mass spectrometry).

The ionic strength (I) is known to influence the double layer thickness and colloidal suspension stability [18]. SWCNT could be affected by an increase in ionic strength because the risk of aggregation is more important then. Additionally, it could be expected for the longest SWCNT located close to the membrane that a too high ionic strength could also induce adsorption onto the membrane. As a consequence of these effects, in this study no SWCNT signal was observed over 10^{-3} mol L^{-1}. Consequently, the ionic strength was tested from 0 to 10^{-3} mol L^{-1}. For a given ionic strength value, pH was studied over the range 6–10, the minimum value corresponding to the pH of SWCNT aqueous suspension and 8–10 being the usual pH range in FlFFF. However, over pH 8 no signal was observed. It could be assumed that at these pH values, some changes in nanotube surface charge could occur. So, aggregation or sorption onto the membrane could be considered. Later on, pH 8 was chosen as the maximum tested. Ionic strength and pH were investigated by performing each run with the channel main flow at 1 mL min^{-1} and the cross-flow value at 0.9 mL min^{-1}. The recoveries obtained are presented in Table 1. It can be noticed that the highest recovery was obtained for an ionic strength of 10^{-5} mol L^{-1} and a pH = 6. Accordingly, these values were chosen as the optimal adjustments. Moreover pH = 6 corresponds to the SWCNT aqueous suspension pH. So no change in carbon nanotube distribution during fractionation due to any change in their surface charge is expected at this pH.

3.1.2. Channel

Channel elements (membrane nature, cut off and spacer) are also crucial parameters in AFlFFF separation because they could directly influence carbon nanotube elution and interactions with the membrane. Three different membrane types were tested: regenerated cellulose (RC), triacetate cellulose (TC), and polyethersulfone (PES). A spacer thickness of 250 μm was first used. The membrane cut off was arbitrary fixed at 10 kDa. The recovery values obtained ranged from 88 to 90% for all these types of membrane. However, regenerated cellulose appears to have less interaction with SWCNT than the two other ones. Indeed, nor peak bending (such splitting or tailing) neither peak retention time increase was observed by using this type of membrane as illustrated in Fig. 2. Moreover the SWCNT lengths obtained using regenerated cellulose membrane correspond to a range (from 125 ± 5 to 1952 ± 10 nm) longer than length ranges obtained with the two other membranes (from 124 ± 9 to 1785 ± 26 nm) and with a maximum length as close as possible to manufacturer one. This shows that possible loss of the longest nanotubes located close to the membrane is minimum with this type

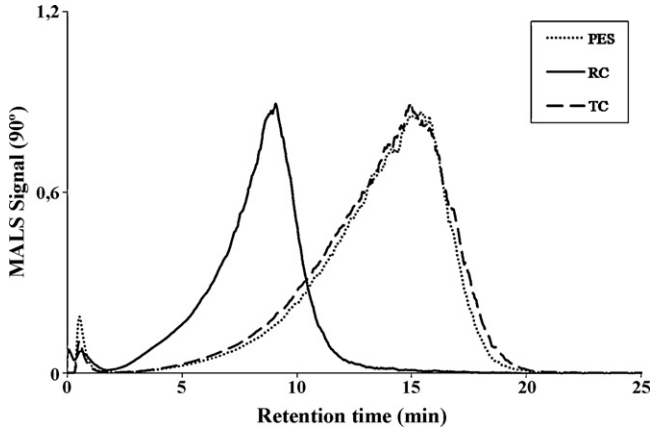

Fig. 2. Typical fractogramms obtained according to different membrane nature (operating conditions: V_c = 0.9 mL min^{-1}, V = 1.0 mL min^{-1}, 10 kDa membrane cut off, 250 μm spacer thickness, injected volume: 100 μL).

of membrane. So, regenerated cellulose membrane was used later on.

Then, different cut off values were tested: 3, 5, 10, 20 and 30 kDa, respectively. No difference between the recoveries obtained from these 5 membrane cut off was observed. For further analysis a regenerated cellulose membrane was chosen, with a cut off of 10 kDa. This cut off was considered as a satisfactory compromise with regard to analyte recovery and channel pressure, channel overpressure being usually observed with a membrane cut off lower than 10 kDa.

Finally spacer thickness was studied because it is known to determine elution profile and can influence analyte membrane interaction. Three different spacer thicknesses were tested: 190, 250 and 350 μm and the results are presented in Fig. 3. The 250 μm spacer allows the retention times to be out of void time and satisfactory analysis duration. Additionally the longest range of SWCNT (from 121 ± 5 to 1941 ± 11 nm) is obtained with this spacer. So 250 μm spacer was used later on.

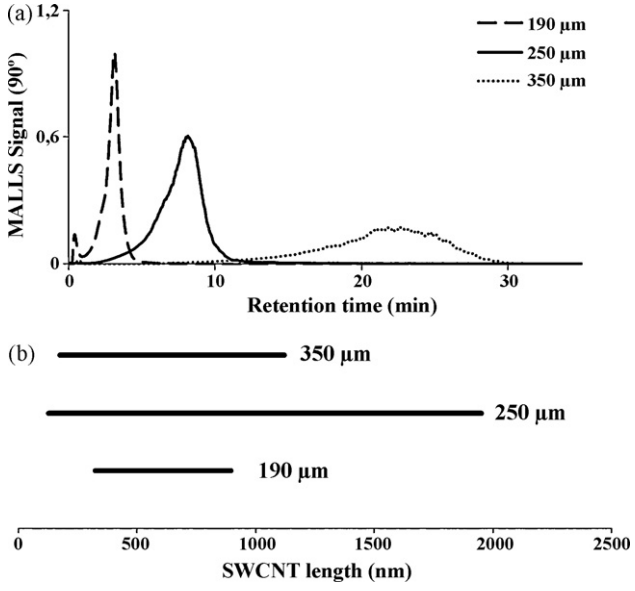

Fig. 3. (a) Typical fractogramms and (b) length ranges (evaluated from 6 replicated analyses, mean RSD = 5%) obtained according to different spacer thicknesses (operating conditions: V_c = 0.9 mL min^{-1}, V = 1.0 mL min^{-1}, regenerated cellulose membrane with 10 kDa cut off, injected volume: 100 μL).

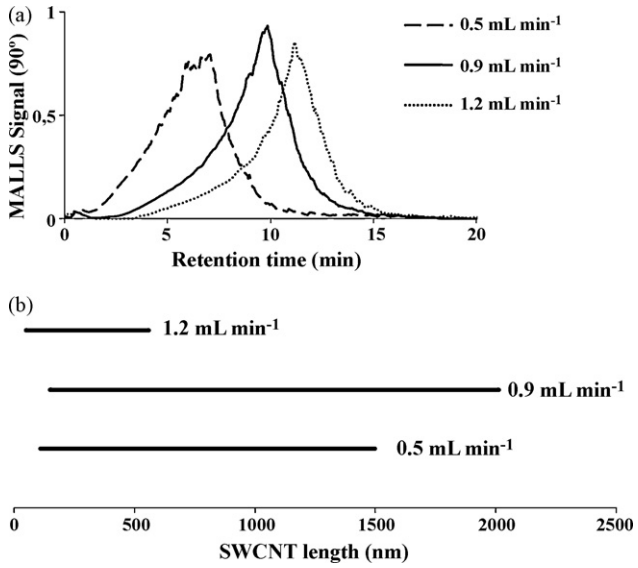

Fig. 4. (a) Selected typical fractogramms and (b) length ranges (evaluated from 6 replicated analysis, mean RSD = 7%) according to different cross-flow rates (operating conditions: V = 1.0 mL min^{-1}, regenerated cellulose membrane with 10 kDa cut off, 250 μm spacer thickness, injected volume: 100 μL).

3.1.3. Cross-flow

If the mobile phase has a major influence on the recovery, the main parameter that controls particle distribution along the channel is the cross-flow rate [32]. On the one hand, a too weak cross-flow does not allow an effective fractionation separation. Then, the shortest nanotubes may be eluted too quickly and partly leave the channel in the void volume. On the other hand, a too strong cross-flow increases the risk of interactions of the analytes with the membrane. Then, irreversible adsorption of the longest nanotubes onto the membrane may be expected. Different cross-flow rates were tested over the range 0.3–1.2 mL min^{-1}. Fig. 4 shows the influence of cross-flow rate on the SWCNT fractionation. A cross-flow rate of 0.9 mL min^{-1} appears to give the longest range of SWCNT (from 119 ± 8 to 1942 ± 21 nm) (see Fig. 4b). Thus, this cross-flow allows the minimum length obtained to be the same as this one found with higher cross-flow and the maximum length to be as close as possible to manufacturer one. Moreover, the fractionation peak is well separated from the void volume (Fig. 4a). Thus any fractionation disturbance due to non-separated particles eluting in the void volume can be avoided. Increasing the cross-flow probably leads to higher interactions of analytes with the membrane and affects the fractionation as the length range becomes very narrow and the maximum length widely decreases over 0.9 mL min^{-1} as showed in Fig. 4. All these results indicate that 0.9 mL min^{-1} represents a satisfactory cross-flow compromise in order to avoid as much as possible any size discrimination due to specific loss.

3.2. Analytical performances

The aim of this part is to evaluate the SWCNT fractionation quality.

Fractionation quality was determined from the test sample. Fig. 5 represents a typical fractogram of this sample obtained in optimized conditions. The quality of fractionation was evaluated by considering three criteria: recovery (representativeness of the sample fractionated), repeatability (from six replicated analyses) and effectiveness of the fractionation. Effectiveness can be estimated taking into account the linearity of the relationship between hydrodynamic radius and retention times (formula (3)) and evaluated by the selectivity (formula (4)). Hydrodynamic radii were experimen-

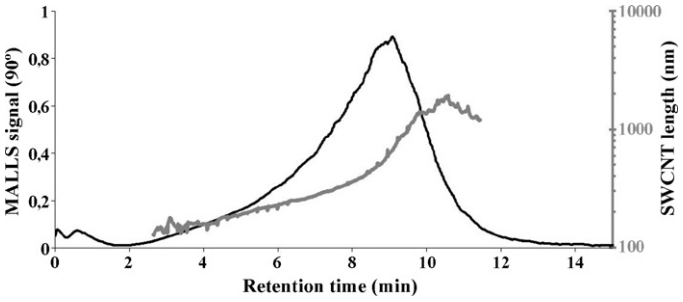

Fig. 5. Typical AFlFFF fractogram of SWCNT with length distribution (from 6 replicated analyses) obtained in selected operating conditions (see the text) (operating conditions: $V_c = 0.9\,mL\,min^{-1}$, $V = 1.0\,mL\,min^{-1}$, regenerated cellulose membrane with 10 kDa cut off, 250 μm spacer thickness, injected volume: 100 μL).

tally measured by DLS from several fractions collected after AFlFFF separation over the detected MALS signal range. By this way, R_h was measured under purely diffusing conditions. Additionally they were evaluated from R_g measurements, by using the formula 12. R_h was also calculated from standard-nanosphere calibration, as usually performed [18,33]. By this approach hydrodynamic radii from FlFFF retention times were determined under fluidic conditions and have to be considered as a sphere-equivalent size evaluation. Complementary, DLS measurements allowed the confirmation that no aggregate was present and SWCNT population was monomodal in eluted sample.

The average recovery was 89 ± 3%. It was obtained with no significant difference in the retention times (maximum of the MALS peak at 8.2 ± 0.2 min), which shows the repeatability of the fractionation. SWCNT hydrodynamic radii versus retention times can be fitted by the following linear curve:

$$R_h = 7.51 \times t_R - 1.32 \quad (13)$$

from DLS measurements, with $R^2 = 1.000$ and $F_{obs} = 1.74 \times 10^{33}$ over 100–1000 nm range. R_h evaluated from R_g measurements and also plotted as a function of t_R leads to a statistically similar fitting. Additionally, these results also confirm that light scattering signal treatment used and Zimm formalism at selected angles are consistent.

Nanosphere hydrodynamic radii (40, 80, 200 and 300 nm) versus retention times are fitted by:

$$R_h = 35.58 \times t_R - 5.14 \quad (14)$$

with $R^2 = 0.9965$ and $F_{obs} = 570$.

These fittings were statistically validated as they were found to be precise (R^2 equal or close to 1), significant ($F_{obs} > F_{\alpha,1,n-1} = 10$, with $\alpha = 0.05$ and $n = 4$) and without bias (no auto-correlated residues).

The selectivity S_d was found to be 0.98 ± 0.02 for SWCNT and 0.97 ± 0.02 for nanospheres as illustrated in Fig. 6. SWCNT selectivity is among the highest values calculated from literature and ranged between 0.55 and 1.02 [8,9,18]. These results show that fractionation is effective in the present operating conditions and in the size range investigated [18]. Fractionation selectivity also appears to be no shape-dependant as the same values are obtained from SWCNT and nanospheres. Moreover, according to the different slope values obtained from the different calibration methods used, R_h calibration by using carbon nanotubes themselves and doing an absolute measurement of their hydrodynamic radii by DLS appears as a relevant procedure. Over around 1000 nm SWCNT length, R_h versus t_R deviates from the linearity. Similar tendency is observed for length variation (see Fig. 5). This increase more rapid than expected suggests an elution possibly more or less influenced by steric effects. Such phenomenon was already observed for SWCNT elsewhere [8,9]. Despite this deviation from the linearity, it can be assumed that SWCNT are eluted in normal mode over the whole length range studied (i.e. 100–2000 nm). On the one hand this assumption is first supported by the continuous increase of R_h according to the retention time. It is also supported by the agreement of the hydrodynamic radius values measured by DLS and those evaluated by formula (12), based on a normal mode elution. On the other hand, SWCNT were previously found to elute in normal mode over a wide length range (from some 10 nm up to some μm) [8]. Their elution has been also showed as governed by their diameter and not their length, nanotubes being expected to elute parallel to the accumulation wall, according to nanotube behaviour simulation and mechanism study in FlFFF channel [9,25]. The deviation from the linearity of R_h versus t_R could come from the SWCNT behaviour in the AFlFFF channel as they become longer. Thus, longer are SWCNT, more complex are their motion. So, even if the diffusion phenomenon remains the key factor, possible complex motion of SWCNT could affect their elution.

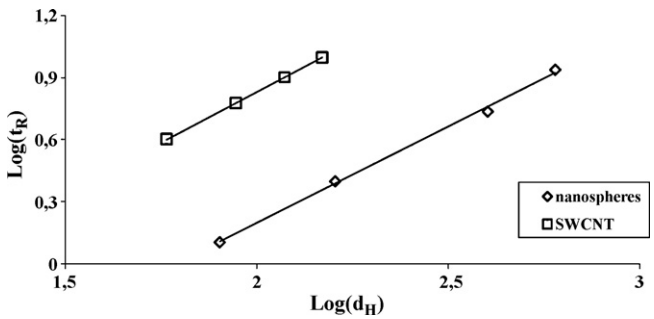

Fig. 6. Logarithm of the retention time (t_R) versus the logarithm of the hydrodynamic diameter (d_H) of nanosphere standards and SWCNT.

The accuracy (i.e. trueness and precision according to the ISO 5725-1) of SWCNT length determination after AFlFFF fractionation was then considered. Trueness was evaluated by first comparing SWCNT lengths obtained by AFlFFF-MALS (Fig. 3) to manufacturer data. From AFlFFF-MALS, SWCNT lengths range from 110 ± 10 to 1942 ± 21 nm, which is in agreement with expected length range. Second, length values from AFlFFF-MALS were compared to those from MALS complementary analysis (direct analysis of bulk test sample without fractionation) in order to evaluate the fractionation reliability. The maximum length appeared to be statistically equal to SWCNT maximum length directly measured by MALS (1955 ± 23 nm) according to a homogeneity test and additionally to the indicative value (2000 nm). Moreover, in order to evaluate AFlFFF-MALS on another length range, the test sample was filtered at 0.45 μm prior analysis. Lengths were found from 112 ± 10 to 478 ± 20 nm, which is in agreement with the expected values. The repeatability of AFlFFF-MALS length determination, evaluated by the mean relative standard deviation (RSD) was 4%. All these results indicate that AFlFFF-MALS provide accurate length determination.

A shape analysis was performed in order to have additional information about the convenience of the whole analytical procedure from fractionation to light scattering measurement and fitting. Such approach consists in combining R_h and R_g values to obtain particle shape factor ρ defined as [31]:

$$\rho = \frac{R_g}{R_h} \quad (15)$$

As it was pointed by Schurtenberger and Newman [31], the determination of ρ gives indication of how far the analyzed particles deviate from the ideal homogeneous sphere ($\rho = 0.775$) to prolate ($\rho > 1$) or oblate ($0.775 < \rho < 1$) ellipsoid.

Fig. 7 presents ρ as a function of the SWCNT length. Two curves were plotted: the first one corresponds to the theoretical

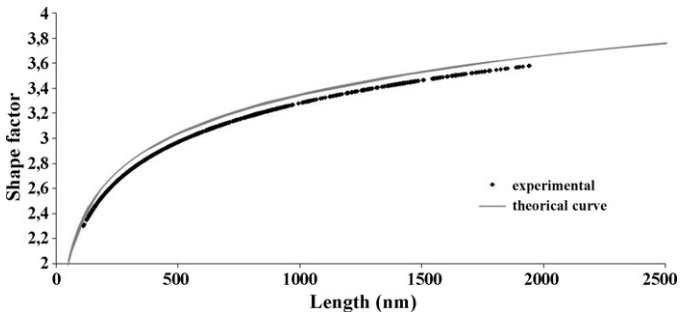

Fig. 7. Shape factor as a function of the SWCNT length.

shape factor plotted by Kammer [33]; the second one represents the experimental shape factor determined from AFlFFF-MALS R_g measurements. The experimental shape factor has values higher than 1.0 (from 2.55 ± 0.08 to 3.95 ± 0.07), which can be conveniently fitted by theoretical ones. These results confirm that prolate ellipsoid model gives a satisfactory SWCNT representation. The agreement of theoretical shape factor to experimental one obtained from SWCNT R_g measurements demonstrated that the methodology presently proposed to achieve SWCNT size information (length and shape factor) is relevant. Finally whole of these results show that AFlFFF-MALS can intrinsically gives an accurate SWCNT length determination.

4. Conclusion

In this work, the capabilities of AFlFFF-MALS were investigated for SWCNT characterisation. Mobile phase (ionic strength and pH) and cross-flow rate appear to act as the major significant parameters controlling SWCNT fractionation. This fractionation appears to be repeatable and occurring in normal mode. SWCNT lengths experimentally determined fit the values obtained without fractionation. This agreement confirms the accuracy of length measurement after AFlFFF on the basis of light scattering modelled by Zimm formalism and assuming SWCNT behave as prolate ellipsoids. These results show the interest to couple AFlFFF with MALS in order to obtain jointly size distribution and length determination. One of the main advantages of AFlFFF-MALS relies on its ability to be coupled to other methods allowing complementary data to be obtained. So it can be considered as relevant with regard to SWCNT characterisation challenge.

References

[1] F. Hennrich, C. Chan, V. Moore, M. Rolandi, M.J. O'Connell, in: M.J. O'Connell (Ed.), Carbon Nanotubes: Properties and Applications, Taylor & Francis, Boca Raton, 2006, p. 1.
[2] B.J. Bauer, M.L. Becker, V. Bajpai, J.A. Fagan, E.K. Hobbie, K. Migler, C.M. Guttman, W.R.J. Blair, J. Phys. Chem. C 111 (2007) 17914.
[3] B.J. Bauer, J.A. Fagan, E.K. Hobbie, J. Chun, V. Bajpai, J. Phys. Chem. C 112 (2008) 1842.
[4] E. Farkas, M. Elizabeth Anderson, Z. Chen, A.G. Rinzler, Chem. Phys. Lett. 363 (2002) 111.
[5] X. Huang, R.S. McLean, M. Zheng, Anal. Chem. 77 (2005) 6225.
[6] M. Zheng, E.D. Semke, J. Am. Chem. Soc. 129 (2007) 6084.
[7] S.K. Doorn, R.E. Fields Iii, H. Hu, M.A. Hamon, R.C. Haddon, J.P. Selegue, V. Majidi, J. Am. Chem. Soc. 124 (2002) 3169.
[8] B. Chen, J.P. Selegue, Anal. Chem. 74 (2002) 4774.
[9] J. Chun, J.A. Fagan, E.K. Hobbie, B.J. Bauer, Anal. Chem. 80 (2008) 2514.
[10] M.H. Moon, D. Kang, J. Jung, J. Kim, J. Sep. Sci. 27 (2004) 710.
[11] H. Peng, N.T. Alvarez, C. Kittrell, R.H. Hauge, H.K. Schmidt, J. Am. Chem. Soc. 128 (2006) 8396.
[12] N. Tagmatarchis, A. Zattoni, P. Reschiglian, M. Prato, Carbon 43 (2005) 1984.
[13] T. Belin, F. Epron, Mater. Sci. Eng. B 119 (2005) 105.
[14] M.S. Dresselhaus, G.G. Samsonidze, S.G. Chou, G. Dresselhaus, J. Jiang, R. Saito, A. Jorio, Physics E 29 (2005) 443.
[15] M.J. O'Connell, S. Sivaram, S.K. Doorn, Phys. Rev. B: Condens. Matter Mater. Phys. 69 (2004) 235415–235421.
[16] D.W. Schaefer, J.M. Brown, D.P. Anderson, J. Zhao, K. Chokalingam, D.W. Tomlin, J. Ilavsky, J. Appl. Crystallogr. 36 (2003) 553.
[17] D.W. Schaefer, J. Zhao, J.M. Brown, D.P. Anderson, D.W. Tomlin, Chem. Phys. Lett. 375 (2003) 369.
[18] M.E. Schimpf, K.D. Caldwell, J.C. Giddings, Field-Flow Fractionation Handbook, Wiley Interscience, New York, 2000.
[19] J. Gigault, I. Le Hécho, S. Dubascoux, M. Potin-Gautier, G. Lespes, Carbon nanotube separation and characterisation based on asymmetrical flow-field flow fractionation couplet to multi-detection, in: Euroanalysis 2009, Innsbruck, Austria, September, 2009.
[20] M. Baalousha, F.V.D. Kammer, M. Motelica-Heino, H.S. Hilal, P. Le Coustumer, J. Chromatogr. A 1104 (2006) 272.
[21] F.V.D. Kammer, M. Baborowski, K. Friese, Anal. Chim. Acta 552 (2005) 166.
[22] M. Andersson, B. Wittgren, K.G. Wahlund, Anal. Chem. 75 (2003) 4279.
[23] R. Pecora, J. Nanopart. Res. 2 (2000) 123.
[24] S Dubascoux, F.V.D. Kammer, I. Le Hecho, M.P. Gautier, G. Lespes, J. Chromatogr. A 1206 (2008) 160.
[25] F.R. Phelan Jr., B.J. Bauer, Chem. Eng. Sci. 62 (2007) 4620.
[26] M.J. Green, N. Behabtu, M. Pasquali, W.W. Adams, Polymer 50 (2009) 4979.
[27] M.L. Monsfield, J.F. Douglas, Macromolecules 41 (2008) 5422.
[28] E.T. Whittaker, A Treatise on the Analytical Dynamics of Particles and Rigid Bodies, 4th ed., Cambridge University Press, New York, 1988.
[29] H.G. Elias, Macromolecules: Physical Structures and Properties, Wiley-VCH, Weinheim, 2008.
[30] F.J. Perrin, Phys. Radium 7 (1936) 1.
[31] P. churtenberg, M.E. Newman, in: J. Buffle, H.P. van Leeuwen (Eds.), Environmental Particles, Vol. 2, IUPAC Environmental Analytical and Physical Chemistry Series, Lewis Publishers, Boca Raton, 1993, p. 37.
[32] R.L. Hartmann, S.K.R. Williams, J. Membr. Sci. 209 (2002) 93.
[33] F.V.D. Kammer, Characterization of Environmental Colloids Applying Field-Flow Fractionation-Multi Detection Analysis with Emphasis on Light Scattering Techniques, Technical University of Hambourg, Harburg, 2004.